Jurnal
Teknologi

Full Paper

CHARACTERISATION OF NANOCRYSTALLINE DIAMOND COATING DEPOSITED VIA HOT FILAMENT CHEMICAL VAPOUR DEPOSITION METHOD WITH VARIOUS SEEDING METHODS

Article history
Received
2 July2014
Received in revised form
6 April 2015
Accepted
1 July 2015

T. M. Yong, E. Hamzah*, M. A. Mat Yajid

Faculty of Mechanical Engineering, Universiti Teknologi Malaysia, 81310 UTM Johor Bahru, Johor, Malaysia

* Corresponding author
esah@fkm.utm.my

Graphical abstract

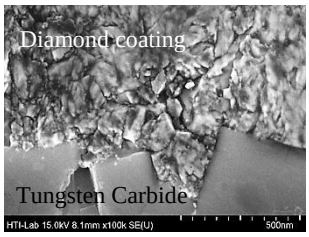

Abstract

A nanocrystalline diamond bilayer has been deposited via hot filament chemical vapour deposition method. The bilayer has been produced by two different deposition parameters. The first is by limiting microcrystalline diamond growth and the second layer by pulsing additional oxygen gas into the system. The two layers become indistinguishable after the deposition ends. The pretreatment of the substrate, tungsten carbide has been varied i.e. its various seeding sizes (<0.1 µm synthetic, <0.5 µm synthetic, <0.25 µm natural, <0.5 µm natural, and <1 µm natural); with and without hammering by silicon carbide. This set up is highly similar to that of previous work however the different deposition time has caused the microcrystalline diamond layer to be nanocrystalline diamond instead. Results presented are the optical and SEM (up to 100,000x magnification) images of both planar and cross-section of the diamond layer. AFM gave topographical analysis of the diamond layer. The results show that the thickness is about 1.7 µm, top layer diamond about 100 nm in size and are indeed diamonds by XRD and Raman.

Keywords: Nanocrystalline diamond, diamond multilayers, characterization, HFCVD, tungsten carbide

Abstrak

Dwilapisan nanokristal intan (berlian) telah diendapkan menggunakan kaedah pengendapan wap kimia filamen panas. Dwilapisan ini telah dihasilkan menggunakan dua jenis parameter enapan. Parameter pertama melibatkan pengehadan pertumbuhan mikrokristal dan parameter kedua melibatkan pendenyutan gas oksigen ke dalam sistem. Kedua-dua lapisan tidak dapat dibezakan selepas proces pengenapan selesai. Parameter pra-rawatan telah diubah iaitu pelbagai saiz benih (<0.1 µm sintetik, <0.5 µm sintetik, <0.25 µm semulajadi, <0.5 µm semulajadi, and <1 µm semulajadi); dengan atau tanpa ketukan karbida silikon, telah digunakan. Penyediaan ini amatlah serupa dengan kajian sebelum ini tetapi masa enapan yang berbeza telah menyebabkan lapisan mikrokristal berubah menjadi lapisan nanokristal. Hasil kajian ini ditunjukkan melalui imej optikal dan SEM (pembesaran sehingga 100,000x) bagi arah pandangan pelan dan keratan rentas lapisan intan. Manakala AFM memberikan analisa topografik lapisan intan. Hasil kajian menunjukkan ketebalan lapisan adalah 1.7 µm, saiz kristal intan adalah 100 nm dan hasil enapan telah dipastikan oleh XRD dan Raman adalah intan.

Kata kunci: Nanokristal intan (berlian), intan (berlian) dengan pelbagai lapisan, HFCVD, karbida tungsten.

1.0 INTRODUCTION

Nanocrystalline diamonds (NCD) films grown on tungsten carbide substrates prove to effectively improve the performance of cutting tools [1-3]. Other than that, NCD films have extensive possible applications in thermal management [4, 5], MEMS, dental [3], tribology, electrochemistry, acoustics, microsensors, cutting tools etc [2, 6]. This is due the fact the NCD have very similar properties of that of a single crystal diamond [7]. The NCD microstructure of ballas morphology has been described as nearly pure diamond with nanocrystalline structure and is caused by high amount of twins and stacking faults [8, 9]. NCD films are mainly grown by manipulating the parameters used for growing microcrystalline diamond (MCD), an earlier and courser form of the diamond film, in various types of chemical vapour deposition machines [10].

Seeding is a process to enhance the nucleation density of the diamond grains that forms the coating. It does this by scratching the surface forming favourable nucleation sites, and it itself broken down during the agitation and implanted into the substrate as actual seeds for growth during the deposition process [11]. Various seeding methods include nanoseeds [12], nano bombardment etc were done by previous researchers.

In this work, a two stage deposition was carried out using both CH_4/H_2 and $CH_4/O_2/H_2$ systems in a hot filament chemical vapour deposition (HFCVD) machine. The results published are part of an on-going parameter manipulation of the HFCVD to achieve better NCD microstructure. Previous work is given in [11, 13, 14].

2.0 EXPERIMENTAL

Tungsten carbide (WC) substrates were prepared but cutting from a rod to <1mm thick. The substrates were treated with Murakami agent, acid solution of HNO_3 and H_2O_2 in 1:9 ratio; and seeded as showed in Table 1 in an ultrasonic bath. WC was selected for it itself is a well-known cutting material and the material promotes nucleation of diamond [15]. Hammering mixture was prepared using Tikapur, water, diamond powder and SiC powder of about 100 µm in size; of 20ml:180ml:0.8g/l:5g/l ratio. The mixture was mechanically stirred and then ultrasonic mixed for 20 minutes prior seeding. Seeding was then done; with or without hammering; by submerging the substrates in an ultrasonic bath of a mixture of Tikapur, water and choice of diamond powder in a 20ml: 180ml: 0.8g/l ratio for 4 minutes. Results of surface cobalt were shown to be well under 1%. This is important as cobalt is a graphite promoter [10]. The prepared substrates then underwent diamond deposition with parameters as shown in Table 2. HFCVD is probably the simplest and most reproducible way to grow diamond at low pressure [10]. These parameters were chosen because the previous batch of diamond coating [14] shows obvious two layer deposition of NCD on MCD. The increase of methane concentration in second stage of deposition increases secondary nucleation rate as a result of increased in carbon species concentration [12]. NCD has preferred properties in comparison to MCD [5]. However MCD show better adhesion [16]. Thus the MCD growth was constrained by manipulating the current deposition parameters. Sample preparation for analysis was done using Struers MD system. Analysis was done using scanning electron microscope (SEM), grazing angle x-ray diffractometer (XRD) at 2°, atomic force microscopy (AFM) and Raman spectroscopy. Raman laser wavelength used was 516 nm.

Table 1 Sample labels and pretreatments

Label	Chemical Pretreatment		Seeding(size & diamond type)	Hammering
	Murakami	Acid		
DA, DK	20 minutes	60 Sec	<0.1 µm synthetic	x
DB, DL			<0.5 µm synthetic	
DC, DM			<0.25 µm natural	
DD, DN			<0.5 µm natural	
DE, DO			<1 µm natural	
DF, DP			<0.1 µm synthetic	√
DG, DQ			<0.5 µm synthetic	
DH, DR			<0.25 µm natural	
DI, DS			<0.5 µm natural	
DJ, DT			<1 µm natural	

Table 2 HFCVD parameters

Parameters	Values	
	Stage 1	Stage 2
Pressure [mPa]	1600	1600
Oxygen [mln]	-	50 mln, Pulsed 16 seconds on 14 seconds off
H2 gas flow rate [mln]	3000	3000
CH4 gas flow rate [mln]	30	88
Filament temperature [°C]	2200	2200
Voltage [V]	60	60
Current [A]	136	136
Filament row 3 & 4 [W/A]	5400	5400
Deposition time [hr]	3	8
Substrate Temperature [°C]	680	680

3.0 RESULTS AND DISCUSSION

Figure 1 shows a coated sample using current deposition parameters. The optical images show a general planar ballas morphology [9], unlike microcrystalline [3], uniformly covering the entire area of the substrate. The cross section image shows a coating layer of 1.7 µm thick and is predicted to be able to provide minimum protection for the substrate [17].

Figure 2, 3 and 4, shows SEM images of taken from cross section and planar surface of sample DA to DI. Figure 2(a) to (c) show sample DI of various magnifications on the planar view. Figure 2(a) shows a partially grinded surface of a cross section. The cross-sectioning process will cause the diamond layer to delaminate about 30 micron from the edge. Failure of the film is by inter-ballas and through inter-NCD grains [7, 11]. Grinding of the exposed WC is done so that SEM analysis of the cross section will show an equal WC and diamond layer height as shown at the left area in Figure 2(a). Figure 2(b) shows a higher magnification of the ballas morphology. It is not until 100,000x magnifications, Figure 2(c) that the NCD can be seen.

Sample DC, DE and DH, Figure 3(a), (c) and (f), show similar microstructure, particle like and larger than NCD gain size. Particles of Figure 3(a) are larger than Figure 3(c) and 3(f). Figure 3(b); sample DD, shows columnar structure of a MCD microstructure. Only Figure 3(d) shows possible NCD microstructure. However the diamond layer being NCD or not will not be concluded here due to disadvantages of SEM imaging. Diamond being very low in atomic weight, needs very low acceleration voltage to be observed. This causes the quality of the image to be compromised. There is also difficulty in sample preparation due to low thickness (1.7 µm) and extreme hardness of diamond itself. Figure 3(e) and (f) of sample DH shows the difference between a fresh fracture surface and a grinded one. The figures show that the grinding process has curved the sharp edges allowing individuality of the grains to be revealed.

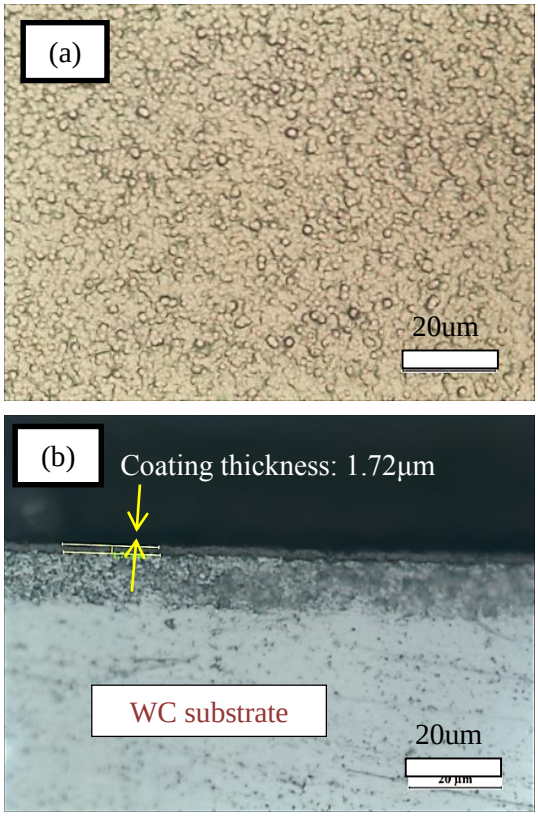

Figure 1 Optical microscope images, (a) planar view (500x), (b) cross section view (500x)

Figure 4, shows a high magnification image of the diamond-substrate interface. It shows that the diamond layer successfully grown in between nicks and valleys of the exposed tungsten carbide substrate. At very high

magnifications, carbon redeposition due to breaking of hydrocarbon contamination on substrate surface is common even though the sample undergone various cleaning procedure. This causes the staining on the sample as seen in Figure 4. However a rough idea of the size of the diamond grain can be seen. It can be generally deduced that while some gains fall in the NCD category, others don't. One reason is that different locations of substrate have different temperature distribution [4] that may even cause morphology changes [11].

The AFM results of sample DD in Figure 5 is sufficient to represent the topography of other coatings of different seeding method since only the surface was accounted. Area scan size 10 µm x 10 µm, 2.5 µm x 2.5 µm and 500 nm x 500 nm were clipped from 20 µm x 20 µm, 5 µm x 5 µm and 1 µm x 1 µm respectively to increase clarity of magnification transition. Figure 6 and Figure 7 show area and line profiles of 10 µm x 10 µm and 500 nm x 500 nm along with their roughness values. From Figure 6, a ballas was estimated to be 2 µm in diameter. Figure 7 shows a wide range of grain size with the large grains slightly larger than the 100 nm NCD defination limit and smaller grains that are under 100 nm. The roughness values of Figure 6 and 7 shows extreme low roughness [18].

Figure 8 and Figure 9, show the XRD results. Diamond peaks along with WC peaks were fully indexed. No other phases were found. The primary diamond peak position is at 2θ, 43.9° was 10 counts lower than that of previous batch [14]. The difference in counts can be easily explained by the thickness of the diamond layer that is, current batch is only 1.7 µm thick in comparison to previous batch of 4.5 µm thick. However the intensity trend for all peaks for all different seeding methods was similar to that of [14]. While there is no 91° diamond peak for without hammering samples, there are some counts for samples with hammering. This suggest that hammering has brought forward, albeit little, the detection of the diamond (331) planes.

In regards of the intensity trends of WC and diamond peaks, it is noted that the diamond peaks have about same intensity, however the WC intensities varies from one seeding method to another. Since WC intensity is collected from the same substrate used for all samples, the cause of this variation must be contributed by the diamond layer as the X-Ray penetrates the diamond layer before penetrating into the WC. Relative intensity ratios show that sizes of natural and synthetic diamond seeds have opposite effects on WC carbide intensity i.e. better crystalinity for smaller natural seeds and larger synthetic seeds. However the seed size for these natural and synthetic seed are about the same size (<0.25 µm and <0.5 µm), thus it could have been perhaps, the extreme size of <0.1 µm synthetic seeds and <1 µm natural seeds that stunt the growth of diamond crystals thus leading to observation of higher WC intensity peaks instead. For the 1 µm seeds, they are relatively easy to be blown off after pretreatment as they have low surface to volume ratio, thus does not adhere to the substrates. This leads to nucleation of diamond to be strictly dependent on the deposition parameters instead nucleation aided by the seeds. For the <0.1 µm seeds, due to sheer size, simultaneous etching and diffusion into substrate during deposition may be the cause of seeds not functioning as nucleuses during deposition [10, 19]. Hammering has an effect on natural seeds. It is postulated that the ultrasonic agitation of SiC breaks down the larger diamond seeds. This causes the intensity ratios for all natural seed size with hammering to be similar. This does not occur with synthetic diamonds most probably because synthetic diamonds were made from larger natural diamond particles to produce the synthetic diamond seeds and cannot be further broken down.

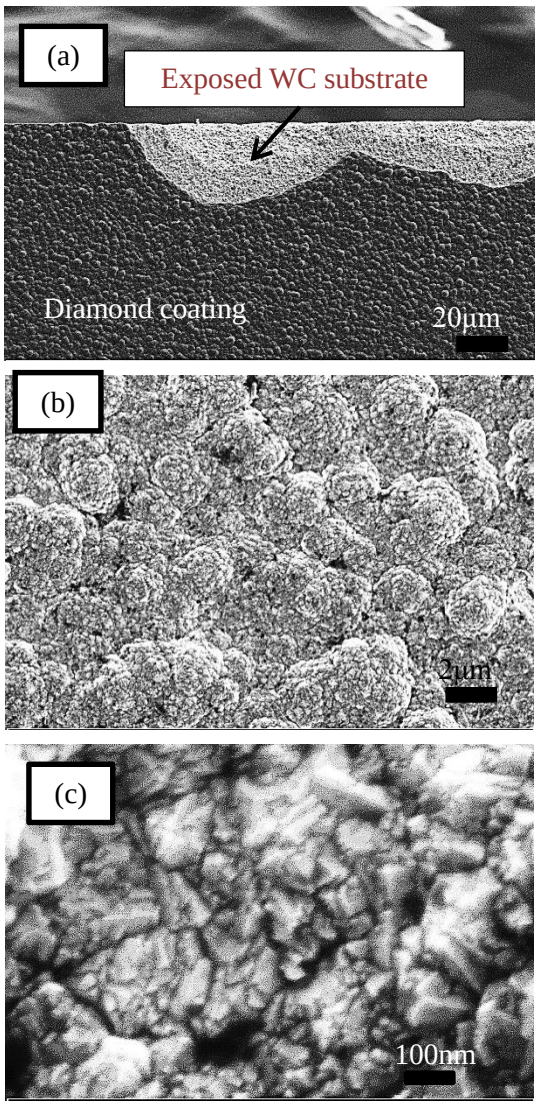

Figure 2 FESEM micrographs of diamond coatings (a) fractured surface, planar view, x 500, (b) Planar view, x 5000, (c) Planar view, x 100 000

Figure 10 shows the Raman Spectra to represent all different seeding method of current deposition as Raman data was taken from the very top layer [14]. Ballas diamond has strong background intensity [8].

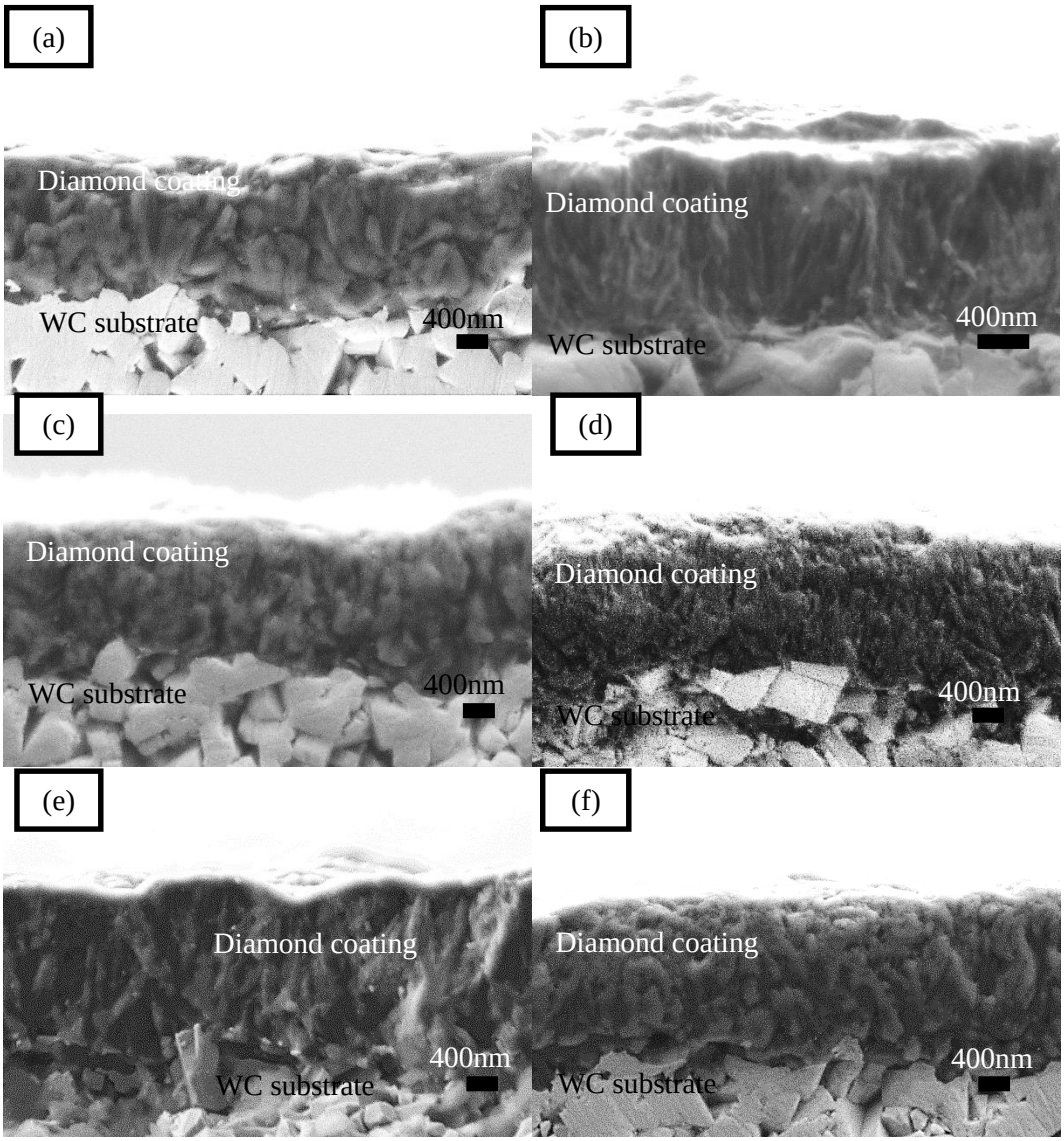

Figure 3 FESEM micrographs of diamond cross-section of current batch (a) x 15 000, (b) x 25 000, (c) x 15 000, (d) x 15 000, (e) fracture surface of cross-section, x 15 000, and (f) grinded surface of cross-section, x 15,000

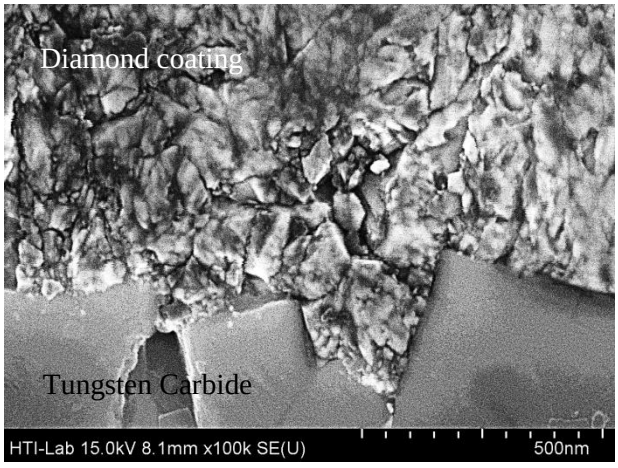

Figure 4 Sample DA (x 100 000)

The raw Raman spectra have been treated. The peak searched and fitted curves made by the software have been omitted as the curves confuses with the corrected Raman spectra that is shown in Figure 10.

The non-presences of first-order 1332 cm^{-1} peak for bulk diamond is reasoned with being overshadowed by the 1343.10 cm^{-1} peak that represents a zone-edge A_{1g} mode that corresponds to Disordered (D) peak [20, 21]. The peak 1137.93 cm^{-1} and 1490 cm^{-1} peak (within the 1534.48 cm^{-1} broad band) corresponded to *trans*-polyacetylene segments which is always present at the grain boundaries of NCD surface [1, 21-23]. However the graphite (G) peak, 1580 cm^{-1}, representing the high frequency E_{2g} first-order mode or 1550cm^{-1} was also suspected to be present in all samples within the 1534.48 cm^{-1} broad band [20, 21]. Presence of graphite formation is common in high defect areas especially boundaries [8].

In contrast with Raman spectra from previous batch that has significant amount of MCD, the NCD identifying peak was a strong and sharp peak shown in Figure 10. This shows better presences of NCD in current batch. However due to the increase in grain boundaries in NCD structure there is an increase of inclusions of non-diamond phases [24]. Thus graphite is suspected to be present in current unlike in previous batch.

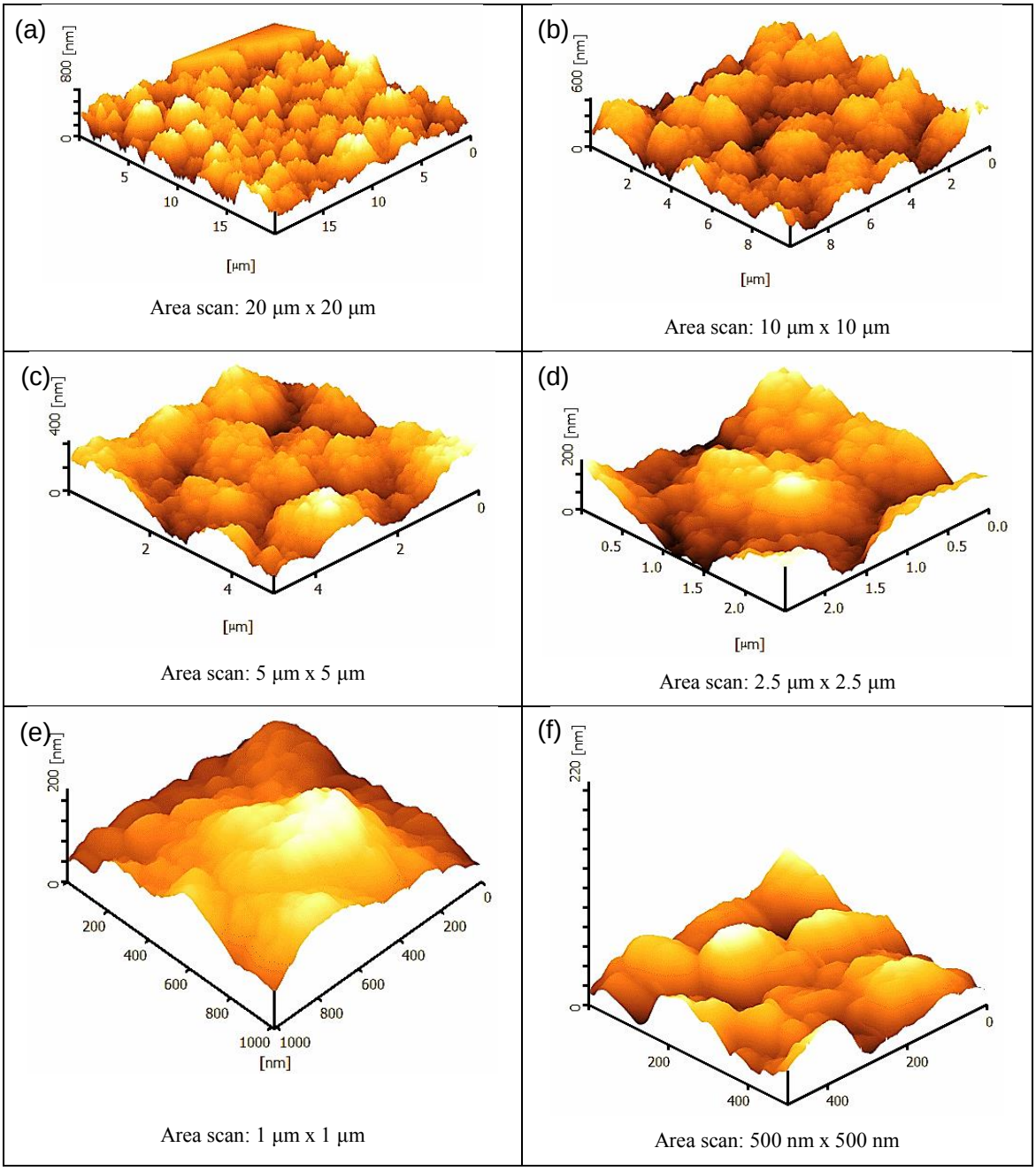

Figure 5 3D topographical view diamond coating of different scan size

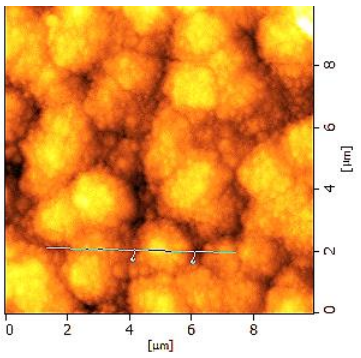

(a)

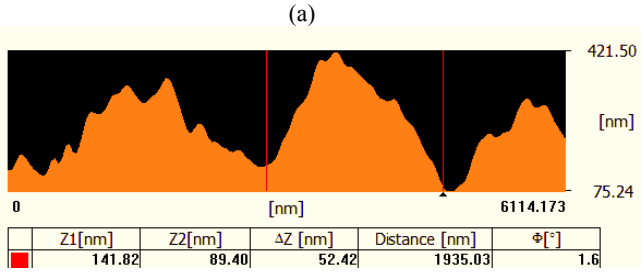

(b)

Label	Value
Ra	83.86 nm
P-V	629.1 nm
Rp	371.2 nm
Rv	-257.8 nm
RMS	100.7 nm
Rz	391.8 nm
S	1.073 x 10^8 nm^2
S Ratio	1.09393

(c)

Label	Value
Ra	29.97 nm
P-V	350.9 nm
Rz	197.7 nm
L	6066 nm
λc	2022 nm
Δa	16.36°

(d)

Figure 6 Diamond coating of 10 µm x 10 µm scan area (a) area profile, (b) line profile, (c) area roughness and (d) Line roughness

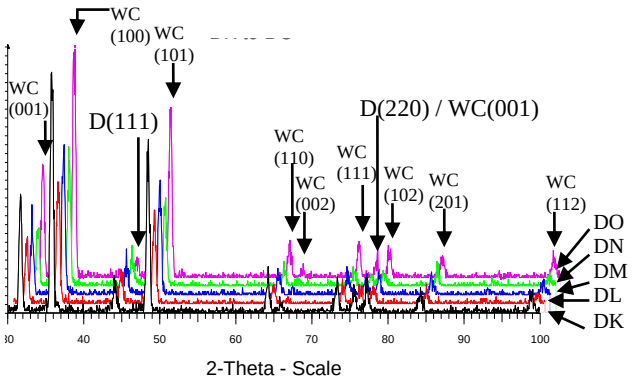

Figure 8 XRD result for diamond coating of Batch C of seeding treatment without hammering

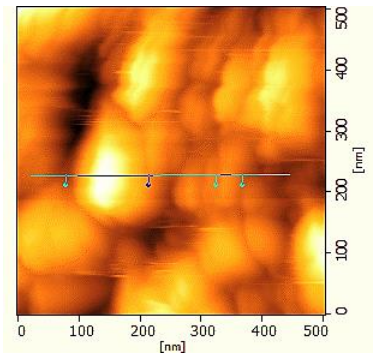

(a)

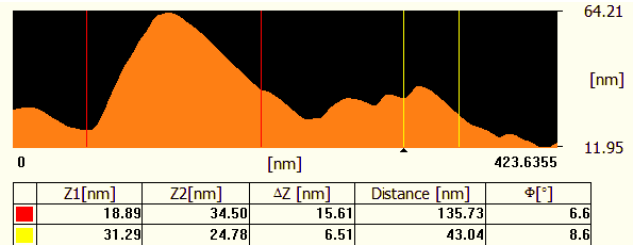

(b)

Label	Value
Ra	9.511 nm
P-V	64.22 nm
Rp	32.71 nm
Rv	-31.51 nm
RMS	11.76 nm
Rz	39.72 nm
S	2.895 x 10^5 nm^2
S Ratio	1.14833

(c)

Label	Value
Ra	2.718 nm
P-V	48.33 nm
Rz	25.77 nm
L	420.3 nm
λc	140.1 nm
Δa	19.06°

(d)

Figure 7 Diamond coating of 500 nm x 500 nm scan area (a) area profile, (b) line profile, (c) area roughness and (d) Line roughness

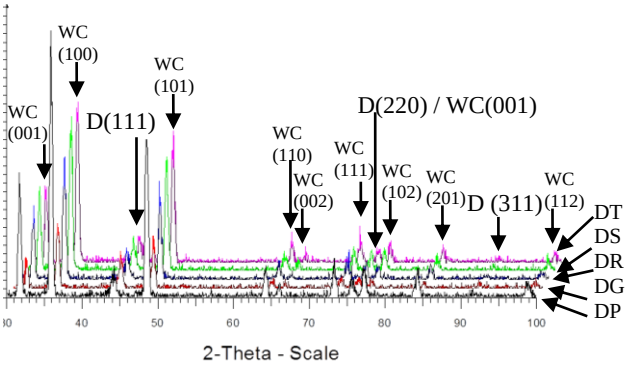

Figure 9 XRD result for diamond coating of Batch C of seeding treatment with hammering

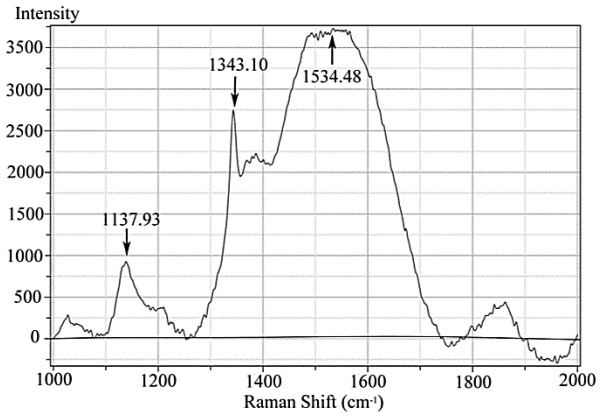

Figure 10 Raman spectrum of diamond coating in current batch

4.0 CONCLUSION

Nanocrystalline diamonds were deposited by HFCVD proven to be as claimed by SEM, AFM, XRD and Raman Spectroscopy. Low magnifications showed the diamond grains were arranged in ballas morphology with 1.7 µm thickness with no MCD diamond columnar grains unlike our previous work [14]. Results from low magnification SEM are inconclusive due to limitation of equipment showing various cross section morphologies. The high magnification cross sectional SEM image shows a mixture of NCD and larger than NCD grains in the diamond coating. This corresponds with AFM results that are more conclusive of the grain size at the surface. The AFM results also confirmed the ballas morphology topography and extreme low roughness of Ra, 83.86 nm of the NCD coating. The XRD proves the non-presence of graphite and diamond-like carbon phases. It also showed that better diamond crystalinity for samples deposited using smaller natural seeds and larger synthetic seeds. Hammering was postulated to break down larger natural seeds and enabled the diamond (311) planes to be detected in XRD. Finally, Raman spectroscopy identified the presence of NCD and graphite. Graphite was assumed to be very low in quantity thus not detected by XRD.

Acknowledgement

The authors would like to thank Ministry of Education Malaysia and Universiti Teknologi Malaysia (UTM) for providing financial support under Research University Grant no. Q.J130000.2524.03H33 and research facilities.

References

[1] Meng, X. M., *et al.* 2008. *International Journal of Refractory Metals and Hard Materials.* 26: 485-490.
[2] Hintermann, H. E. 1996. Advances and development in CVD technology. *Materials Science and Engineering A*. 209: 366-371.
[3] Sein, H., *et al.* 2004. Performance and Characterisation of CVD Diamond Coated, Sintered Diamond and WC-Co Cutting Tools for Dental and Micromachining Applications. *Thin Solid Films.* 447-448: 455-461.
[4] Glaser, A., *et al.* 2006. Deposition of Uniform and Well Adhesive Diamond Layers on Planar Tungsten Copper Substrates for Heat Spreading Applications. *Materials Science and Engineering: B.* 127: 186-192.
[5] Coe, S. E. and R. S. Sussmann. 2000. Optical, Thermal and Mechanical Properties of CVD Diamond. *Diamond & Related Materials*. 9: 1726-1729.
[6] O. A. Williams, M. N., M. Daenen, S. Michaelson, A. Hoffman, E. Osawa, K. Haenen, R. B. Jackman., Diam. 2008. *Relat. Mater.* 17: 1080-1088.
[7] Kamiya, S., *et al.* 2000. Fracture Strength of Chemically Vapor Deposited Diamond on the Substrate and Its Relation to the Crystalline Structure. *Diamond & Related Materials.* 9: 1110-1114.
[8] Haubner, R. and B. Lux. 2002. Deposition of Ballas Diamond and Nano-crystalline Diamond. *International Journal of Refractory metals and Hard Materials*. 20: 93-100.
[9] Yan, C.-S. and Y. K. Vohra. 1999. Multiple Twinning and Nitrogen Defect Center in Chemical Vapor Deposited Homoepitaxial Diamond. *Diamond & Related Materials*. 8: 2022-2031.
[10] Schwander, M. and K. Partes. 2011. A Review of Diamond Synthesis by CVD Processes. *Diamond and Related Materials.* 20: 1287-1201.
[11] Hamzah, E., T. M. Yong, and M. A. M. Yajid. 2013. *Journal of Crystal Growth.* 372: 109-115.
[12] Li, H., *et al.* 2009. *Diamond and Related Materials*. 18: 1369-1374.
[13] Hamzah, E. and T.M. Yong. 2012. *Jurnal Teknologi (Sciences & Engineering).* 59: 65-69.
[14] Yong, T. M. and E. Hamzah. 2014. *Advanced Materials Research.* 845: 36-40.
[15] Aoki, Y., Y. Nakamuta, and Y. Sugawara. 1995. Formation of Tetrapod-Like Crystals of Diamond Formed by Hot-Filament Chemical Vapour Deposition: Effects of Preformation of Tungsten Carbide on Substrate. *Journal of Crystal Growth*. 147: 77-82.
[16] Kamiya, S., *et al.* 2000. Quantitative Determination of the Adhesive Fracture Thoughness of CVD diamond to WC-Co Cememted Carbide. *Diamond & Related Materials.* 9: 191-194.
[17] Brookes, C. A., L. Y. Zhang, and P. W. May. 1997. On the Mechanical Integrity Ratio of Diamond Coatings. *Diamond & Related Materials.* 6: 348-352.
[18] Sharda, T., *et al.* 2001. High Compressive Stress in Nanocrystalline Diamond Films Grown by Microwave Plasma Chemical Vapor Deposition. *Diamond & Related Materials*. 10: 352-357.
[19] Hwang, N. M. and D. Y. Yoon. 1996. Thermodynamic Approach to the Paradox of Diamond Formation with Simultaneous Graphite Etching in the Low Pressure of Diamond. *Journal of Crystal Growth*. 160: 98-103.
[20] Barbosa, D. C., et al. 2009. Influence of Substrate Temperature on Formation of Ultrananocrystalline Diamond Films deposited by HFCVD Argon-Rich Gas Mixture. *Diamond & Related Materials.* 18: 1283-1288.
[21] Azevedo, A. F., et al. 2008. Graphitization Effects of CH4 Addition on NCD Growth by First and Second Raman Spectra and by X-Ray Diffraction Measurements. *Diamond & Related Materials.* 17: 1137-1142.
[22] Wei, Q. P., *et al.* 2009. Applied Surface Science. 256: 1322-1328.

[23] May, P.W., *et al*. 2008. Raman and Conductivity Studies of Boron-doped Microcrystalline Diamond, Facetted Nanocrystalline Diamond and Cauliflower Films. *Diamond & Related Materials.* 17: 105-117.

[24] O. A. Williams. 2011. Nanocrystalline Diamond. *Diamond & Related Materials*. 20: 621-640.